Time dependent β-convection in rapidly rotating spherical shells

V. Morin and E. Dormy[a)]
Institut de physique du globe de Paris, 75252 Paris, France

(Received 13 June 2003; accepted 17 February 2004; published online 6 April 2004)

A quasi-geostrophic, or β, model of nonlinear thermal convection in rapidly rotating spherical fluid shells is investigated. We study time dependent instabilities for a range of Rayleigh number and Ekman number with a Prandtl number set to the unity. Above the onset of convection, increasing the Rayleigh number for a given Ekman number, we reproduce the sequence of bifurcations described by Busse [Phys. Fluids **14**, 1301 (2002)] for the three-dimensional case: A first transition results in vacillating flow; a second transition gives rise to chaotic oscillations in time and localized convection in space; then a third leads to quasi-periodic relaxation oscillations. This study shows that the quasigeostrophic model encompasses the desired bifurcation sequence. It allows the investigation of a range of Ekman numbers unavailable to three-dimensional models with present computing resources. Decreasing the Ekman number, we unexpectedly found that all three transitions occur for marginally supercritical Rayleigh number. The range of Rayleigh number for which the amplitude of convection is steady vanishes in the asymptotic limit of small Ekman numbers. This effect could significantly alter the nature of the instability characterizing the onset of convection in particular whether it is a supercritical or subcritical bifurcation. © *2004 American Institute of Physics.* [DOI: 10.1063/1.1703530]

I. INTRODUCTION

Convection in rotating spherical fluid shells is an important problem when seeking to understand of magnetic field generation by self-excited dynamo action in planetary interiors. While this hydrodynamic problem is considerably simpler than the full magnetohydrodynamic scenario, the rapid rotation of these natural objects means realistic modeling is still challenging, even close to the onset. The full description of the linear instability has only been obtained recently,[1] elucidating the issue of the variation of phase velocity with the radius (phase mixing or Taylor diffusion) raised earlier[2] concerning the local treatment of the instability.[3] However, several important issues remain unresolved. In particular, the effects of nonlinearities are expected to counteract phase mixing, and yield a subcritical bifurcation,[2] while numerical simulations have always produced supercritical bifurcations.[4,5]

To study convection in rapidly rotating systems, Busse[3] introduced an annulus model. This model took into account the dominant role of rotation (Taylor–Proudmann theorem) to reduce the problem from three dimensions to two, and used the small gap approximation to further simplify the model. Or and Busse[6,7] modified this two-dimensional approach by introducing parabolic boundaries and thus phase mixing. They studied vacillating oscillations which appear when the Rayleigh number is increased for a fixed and moderate Ekman number. Chen and Zhang,[9] with a two-dimensional model similar to Refs. 6 and 7 but in a finite gap configuration, studied vacillating and chaotic oscillations varying the aspect ratio.

Yano demonstrated analytically[10] that the phase mixing issue can be resolved in a modified version of the cylindrical Busse annulus[3] taking into account the curvature of the boundaries which are essential to phase mixing. Using this configuration he resolved the linear instability problem.

In the light of this earlier work, we propose to use a simplified two-dimensionnal numerical model to study the possible existence of a subcritical bifurcation for the onset of convection. We first describe the sequence of bifurcations which occurs in the nonlinear domain and compare it with the one investigated by Busse and Grote[8] with a fully three-dimensional model in a spherical geometry. Our model is based on the quasi-geostrophic approximation and has spherical boundaries. It is used to obtain insight on the full three-dimensional problem. Since the quasi-geostrophic model is reduced to two dimensions it involves a less demanding numerical integration, and thus allows a larger parameter space survey.

After presenting the quasi-geostrophic model in Sec. II, linear results are detailed in Sec. III A and the results of nonlinear convection are presented in Sec. III B. This is followed by a discussion in Sec. IV.

II. QUASI-GEOSTROPHIC MODEL

We consider motions driven by buoyancy in a rotating spherical shell (i.e., the domain between two concentric spheres) with a uniform distribution of internal heat sources. The rotation rate is Ω, ν is the kinematic diffusivity, κ is the thermal diffusivity, and α the coefficient of thermal expansion. The gravity field is assumed to be $-g\boldsymbol{r}$ which corresponds to a self-gravitating sphere. We introduce θ as the

[a)]Present address: CNRS/UMR8550, Departement de Physique, Ecole Normale Superieure, 24 rue Lhomond, 75231 Paris Cedex 05, France; electronic mail: dormy@lps.ens.fr

deviation from the basic temperature profile of pure conduction: $T_s = T_0 - \tilde{\beta} r^2/2$. The temperature gradient in the absence of convection is thus $-\tilde{\beta} r$.

We define the unit of time to be r_o^2/ν, the unit of length being the outer sphere radius r_o, and the unit of temperature $\tilde{\beta} r_o^2 \nu/\kappa$. We introduced the following dimensionless parameters:

$$E = \frac{\nu}{2\Omega r_o^2}, \quad Ra = \frac{\alpha \beta g r_o^6}{\nu \kappa}, \quad Pr = \frac{\nu}{\kappa}, \tag{1}$$

namely the Ekman number, Rayleigh number, and Prandtl number. The equations of motions (Navier–Stokes) and continuity under the Boussinesq approximation are then

$$\frac{\partial \boldsymbol{u}}{\partial t} = -(\boldsymbol{u}\cdot\boldsymbol{\nabla})\boldsymbol{u} + Ra\,\theta \boldsymbol{r} - \boldsymbol{\nabla}\Pi + \Delta \boldsymbol{u} - E^{-1}(\boldsymbol{e}_z \wedge \boldsymbol{u}), \tag{2}$$

$$\nabla \cdot \boldsymbol{u} = 0. \tag{3}$$

While the temperature perturbation equation is

$$\frac{\partial \theta}{\partial t} = -(\boldsymbol{u}\cdot\boldsymbol{\nabla})\theta + Pr^{-1}(\boldsymbol{u}\cdot\boldsymbol{r} + \Delta\theta). \tag{4}$$

Introducing the axial component of vorticity as ζ, and taking the z-component of the curl of (2), one obtains after averaging in z and neglecting $\overline{\zeta \partial_z u_z}$

$$\frac{\partial \overline{\zeta}}{\partial t} = -(\boldsymbol{u}\cdot\boldsymbol{\nabla})\overline{\zeta} - Ra\,\frac{\partial \overline{\theta}}{\partial \varphi} + \Delta \overline{\zeta} + \frac{E^{-1}}{2H}[u_z]_{-H}^{H}, \tag{5}$$

where $\overline{\zeta} = (1/2H)\int_{-H}^{H} \zeta\, dz$ (H being the half height of a convection column). Following on the cylindrical model of Busse[3] and thus neglecting the z variations of the horizontal component of the velocity, the flow is now assumed to be quasi-geostrophic. Using cylindrical coordinates, this corresponds to approximating both u_s and u_φ with functions that are independent of z, and thus $\overline{\zeta} = \zeta$, while the z variation of u_z obviously cannot be neglected. This implies that the necessary dependance of u_z on z is approximated by a linear variation to satisfy the continuity equation. This approximation can clearly not be fully justified in the case of curved boundaries. It is, however, found to yield remarkably precise results in good agreements with experiments (e.g., Ref. 11). Using the nonpenetration condition at the boundaries, (5) becomes

$$\frac{\partial \zeta}{\partial t} = -(\boldsymbol{u}\cdot\boldsymbol{\nabla})\zeta - Ra\,\frac{\partial \overline{\theta}}{\partial \varphi} + \Delta \zeta - E^{-1}\frac{s}{1-s^2}u_s. \tag{6}$$

Note that this equation, once linearized, is nothing more than Eq. (4.5) in Ref. 3. This includes the last term which is equivalent to the β-plane effect used in meteorology. It accounts for the effect of vortex tube stretching (and shortening) as one moves toward (away) the axis of rotation. This equation can be expressed in terms of stream function ($\boldsymbol{u} = 1/s\ \partial_\varphi \psi \boldsymbol{e}_s - \partial_s \psi \boldsymbol{e}_\varphi$), under the assumption of small vertical variations. Vanishing normal velocity implies that ψ is constant on each boundary, and because ψ is defined to an arbitrary constant, it can be set to zero in the case of a simply connected domain. This is however not the case for our shell geometry. For this reason, and to avoid driving a zonal flow by an erroneous mean pressure gradient (see Ref. 12 for discussion), we write a separate equation for the ϕ-averaged zonal velocity (henceforth denoted by a 0 subscript). All other modes are expressed in terms of the stream function ψ. Taking the z average of equation (4) and neglecting the terms $\overline{u_z \partial_z \theta}$ and $\overline{z u_z}$, one obtains the resulting system of equations:

$$\begin{aligned}
&\left(\frac{\partial}{\partial t} - \Delta\right)\Delta\psi = -(\boldsymbol{u}\cdot\boldsymbol{\nabla})\Delta\psi + \frac{E^{-1}}{1-s^2}\frac{\partial \psi}{\partial \varphi} + Ra\,\frac{\partial \overline{\theta}}{\partial \varphi},\\
&\left(\frac{\partial}{\partial t} - \left(\Delta - \frac{1}{r^2}\right)\right)\overline{u}_0 = -(\overline{(\boldsymbol{u}\cdot\boldsymbol{\nabla})u_\varphi})_0,\\
&\left(\frac{\partial}{\partial t} - Pr^{-1}\Delta\right)\overline{\theta} = -(\boldsymbol{u}\cdot\boldsymbol{\nabla})\overline{\theta} + Pr^{-1}\frac{\partial \psi}{\partial \varphi}.
\end{aligned} \tag{7}$$

The temperature perturbation vanishes at each boundary,

$$\theta = 0, \tag{8}$$

while the velocity satisfies either no-slip or stress-free boundary conditions, respectively,

$$\psi = \frac{\partial \psi}{\partial s} = u_0 = 0 \tag{9}$$

and

$$\psi = \frac{\partial}{\partial s}\left(\frac{1}{s}\frac{\partial \psi}{\partial s}\right) = \frac{\partial}{\partial s}\left(\frac{u_0}{s}\right) = 0. \tag{10}$$

The Prandtl number is here set to unity, and the aspect ratio r_o/r_i is fixed to 0.35 for geophysical relevance. This system corresponds to a modification of the one introduced by Busse[3] for a cylindrical annulus and was also used with a different heating mode, and very far from onset by Aubert *et al.*[11] A similar approach has been used by Or and Busse,[6,7] and Chen and Zhang[9] where they used the annulus model[3] with a first order Taylor expansion of the boundary, but with a finite gap for Ref. 9. They have investigated vacillating oscillations[6,7,9] and chaotic convection.[9] Chen and Zhang[9] have also studied the effect of varying the aspect ratio for a given Ekman number.

The set of equations (7) was discretized in Fourier modes in the azimuthal direction, and with a finite differences method on stretched grids in the radial direction. Diffusion terms, as well as the Coriolis term, were time stepped with a Crank–Nicholson scheme. The nonlinearity and coupling terms were computed with a second order Adams–Bashford scheme. We used two different approaches for evaluating these terms. The first approach consisted in evaluating these terms in physical space using a fast Fourier transform, the second consisted of evaluating explicit mode coupling in the spectral space, and was restricted to two modes only, the mode $m = 0$ and the critical mode m_c. Our numerical code was successfully benchmarked against the independently written code of Aubert *et al.*[11]

TABLE I. Critical parameters for the onset of convection in the quasi-geostrophic model (Pr=1).

E	m_c	Ra_c	ω_c	$m_cE^{1/3}$	$Ra_cE^{4/3}$	$\omega_cE^{2/3}$
			No-Slip			
10^{-4}	7	$6.024\cdot10^5$	272.48	0.325	2.80	0.587
10^{-5}	13	$1.091\cdot10^7$	1179.2	0.280	2.35	0.547
10^{-6}	23	$2.206\cdot10^8$	4967.8	0.230	2.20	0.497
10^{-7}	56	$4.690\cdot10^9$	24571	0.260	2.18	0.529
10^{-8}	122	$9.958\cdot10^{10}$	114185	0.263	2.15	0.530
			Stress-free			
10^{-4}	7	$5.961\cdot10^5$	268.50	0.325	2.77	0.578
10^{-5}	12	$1.086\cdot10^7$	1134.4	0.258	2.34	0.526
10^{-6}	22	$2.215\cdot10^8$	4856.4	0.220	2.21	0.485
10^{-7}	56	$4.690\cdot10^9$	24573	0.260	2.18	0.529
10^{-8}	122	$9.914\cdot10^{10}$	113510	0.263	2.14	0.527

III. ONSET OF CONVECTION AND NONLINEAR REGIME

A. Linear results

To study the onset of convection, we timestep the linearized system (for which the azimuthal modes m are decoupled) until we reach an exponentially growing solution. The critical parameters are obtained through linear interpolation of the growth rate very near the onset (see Ref. 13 for further discussions of this approach). It is to be noted that our linear results are also relevant for a full sphere provided E is small enough (see Ref. 13 for a discussion of the role of the inner core on the onset of convection), this will, however, not be the case in the nonlinear regime because the zonal flow occupies the full domain and is thus affected by the inner body. The onset of convection occurs through a Hopf bifurcation.[3] The imaginary part of the eigenvalue corresponds to the drift rate of the thermal Rossby waves. The critical parameters (unstable mode m_c, Rayleigh number Ra_c, and drift rate ω_c) obtained for our model for both sets of boundary conditions (no-slip and stress-free) are reported in Table I. These results validate the classical asymptotic scalings[3,14] $m_c \propto E^{-1/3}$, $Ra_c \propto E^{-4/3}$, and $\omega_c \propto E^{-2/3}$. We have also checked that the resulting eigenfunctions qualitatively follow the theoretical description of Jones *et al.*[1] (i.e., a Gaussian envelope of scaling $E^{1/6}$ with oscillations of the real and imaginary part of the eigenfunction scaling as $E^{1/3}$), thus demonstrating that phase mixing also occurs for this reduced system, and that the linear solution discussed here is best described in terms of global instability.

B. Nonlinear behavior

1. Fully nonlinear results

Let us first describe the sequence of bifurcations obtained with our two-dimensional model using the fast Fourier transform algorithm. Busse and Grote[8,15,16] describe, with fully three-dimensional simulations and stress free boundary conditions, the consecutive transitions which occur as the Rayleigh number is increased above the onset of convection for a given Ekman number ($E=10^{-4}$ in their case). The first step in the series of transitions is referred to as vacillating oscillations (see Ref. 17 for three-dimensional problems, and Refs. 18 and 19 for two-dimensional cylindrical models). It corresponds to a sinusoidal oscillation in time of the kinetic energy. The azimuthal periodicity of the pattern is conserved, but an oscillation of the shape of the convective region develops. Busse[16] has noticed, by plotting the Nusselt number as a function of Rayleigh number, that the energy dissipation is enhanced through this bifurcation. Several modes become unstable as the Rayleigh number increases. Figure 1 presents oscillations of the kinetic energy, obtained with the quasigeostrophic model for such a parameter regime. This instability is observed with both no-slip and stress-free boundary conditions. The precise value of the control parameter for which this transition occurs depends on the boundary conditions (just as the critical parameters of Table I). The parameters used for Fig. 1 correspond to the lowest values of the Ray-

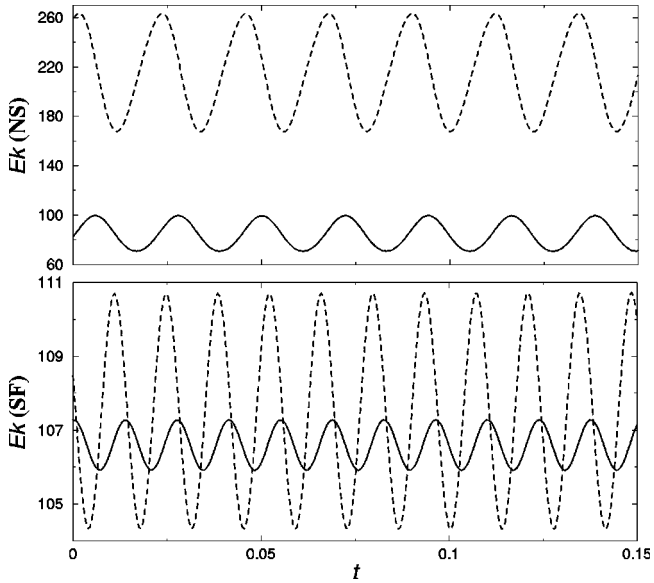

FIG. 1. Time oscillations of the kinetic energy for $E=10^{-5}$, $Pr=1$, and $Ra=1.4\times Ra_c$, with no-slip boundary conditions (top graph), and $Ra=1.34\times Ra_c$, with stress-free boundary conditions (bottom graph). This parameter regime corresponds to vacillating oscillations. The energy of the sum of all nonaxisymmetric modes (Ek') is represented by a dashed line, and the energy of mode $m=0$ (Ek_0) by a solid line. The unit of time is the viscous time scale.

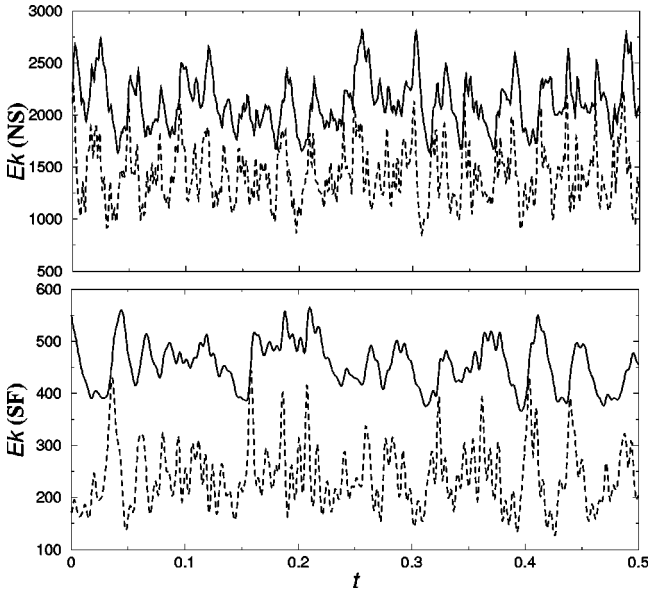

FIG. 2. Time dependent oscillations of the kinetic energy for $E=10^{-5}$, $Pr=1$, and $Ra=2\times Ra_c$, with no-slip boundary conditions (top graph), and $Ra=1.6\times Ra_c$, with stress-free boundary conditions (bottom graph). This parameter regime corresponds to a chaotic time dependence, periodicity is lost. The energy of sum of all nonaxisymmetric mode (Ek') is represented by a dashed line, and the energy of mode $m=0$ (Ek_0) by a solid line. The unit of time is the viscous time scale.

FIG. 3. Isovalues of ψ for $E=10^{-5}$, $Ra=2\times Ra_c$, $Pr=1$, with no-slip boundary conditions. This graph corresponds to chaotic oscillations, the azimuthal periodicity of the pattern is no longer preserved. Patterns of convection are localized by the shearing action of the zonal flow.

leigh number for which a time dependent amplitude was observed. The kinetic energy, Ek, of the horizontal flow has been calculated as the integral over the domain of $(u_s^2+u_\varphi^2)$, the velocity being expressed in units of ν/r_o. This can be separated in two contributions, the energy of the mean zonal flow, Ek_0, which is the integral of $\overline{u_0}$, and the nonaxisymetric energy, Ek', which is the integral of $((1/s\partial_\varphi\psi)^2+(\partial_s\psi)^2)$. The sequence of bifurcations obtained with this model compares extremely well with the earlier three-dimensional results of Busse *et al.*, although the actual values of the parameters for transitions to occur necessarily differ in this reduced model from the full three-dimensional numerical simulations.[8,15,16] When increasing the Rayleigh number, period doubling occurs, as in the three-dimensional study of Ref. 8.

Chen *et al.* have investigated the sequence of bifurcations described by[8,15,16] with their two-dimensional model using no-slip boundary conditions. They have reproduced the first two steps of this sequence, i.e., the vacillating oscillations and chaotic oscillations however they report no indication of the relaxation oscillations, which is consistent with our simulations for a comparable parameter regime. They have investigated the details of the successive transitions in between these bifurcations. They report up to nine transitions which are characterized by enlarging the spatial scale of the convection. We have obtained similar results with our largest Ekman number, but the details of the transition scenario are highly dependent of the Ekman number. A similar enlarging of the spatial scale (i.e., decrease in the dominant wavenumber m) has been observed in our simulations for large enough values of the Ekman number.

Increasing the Rayleigh number further, the azimuthal periodicity of the solution is conserved, but the zonal flow increases in magnitude and strongly shears the convective region. This tends to split the convective cells into a inner and outer ring.

As in Refs. 8, 15, and 16, with a further increase in Rayleigh number, a new bifurcation occurs which is characterized by chaotic oscillations in time of the kinetic energy of the system (see Fig. 2). The azimuthal periodicity of the pattern is no longer preserved and the shearing action of the zonal flow becomes so strong that the convection structures tend to concentrate in a reduced part of the shell. This localized convection is illustrated on Fig. 3.

At higher Rayleigh number, a new transition occurs in the form of quasi-periodic relaxation oscillations in time of the kinetic energy, as pointed out by Grote *et al.*[15] with their three-dimensional model. Spatial periodicity is, however, not recovered. This quasi-periodic relaxation (fairly similar to that observed in zero Prandtl number convection[20]) is due to the presence of a strong zonal shear.[21] As the shear becomes dominant, the convection decays. Eventually, the zonal flow is not sustained anymore, and is suppressed by viscous dissipation. Convection can then restart, and this process repeats almost periodically. The same transition is reproduced with our two dimensional model (see Fig. 4). The effect of boundary conditions is particularly important for this transition as it strongly affects the period of the relaxation oscillations. As convection is suppressed, the mean zonal flow decays by diffusion. It is well known that no-slip boundary conditions will lead to a faster decrease than stress-free (since the zonal flow then vanishes at the boudaries). This is here characterized by a much shorter period of oscillation with no-slip boundary conditions (see also Fig. 8). The period becomes less regular as the Rayleigh number is increased. The energy of the nonaxisymetric modes varies over a range of modes in a time dependent manner.

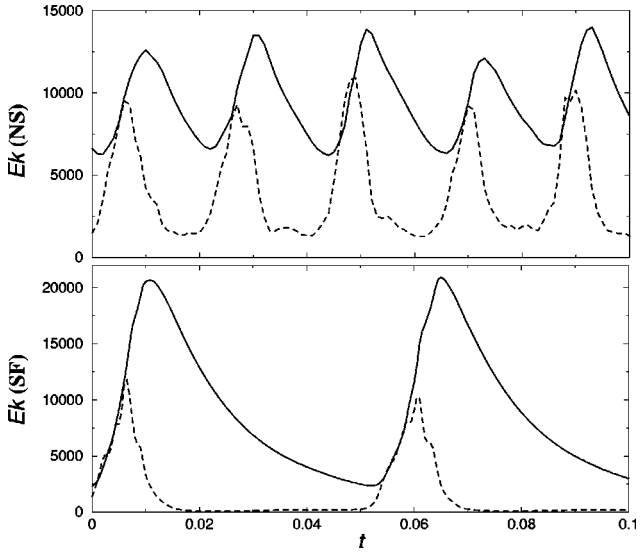

FIG. 4. Time oscillations of the kinetic energy for $E=10^{-5}$, $Pr=1$, and $Ra=3\times Ra_c$, with no-slip boundary conditions (top graph), and $Ra=2.6\times Ra_c$, with stress-free boundary conditions (bottom graph). This parameter regime corresponds to relaxation oscillations. The energy of sum of nonaxisymmetric (Ek') mode is represented by a dashed line and the energy of mode $m=0$ (scaled by 0.5 for top graph) by a solid line. The unit of time is the viscous time scale.

2. Explicit mode coupling results

We have also produced a sequence of bifurcations with a less demanding numerical approach which employs an explicit mode coupling in the spectral domain. This weakly nonlinear model was severely truncated by only computing two modes (the critical mode and the mode $m=0$). Vacillating oscillations are represented on Fig. 5 with no-slip boundary conditions, they appear for a range of Rayleigh number extremely close to that found using much higher spectral resolution and the fast Fourier transform algorithm. This approximation is classical, and well justified for the investigation of nonlinearities very close to the onset. As one applies this approximation further away from the critical value of the Rayleigh number, it becomes less strongly justified, and can only yield qualitative information on the dynamics. For example, while the time dependence is very well reproduced by this model on Fig. 5, comparison with Fig. 1 reveals that the energies differ by a factor of two. This only high-lights the limitations of this very severely truncated model in providing more quantitative informations on the full dynamics.

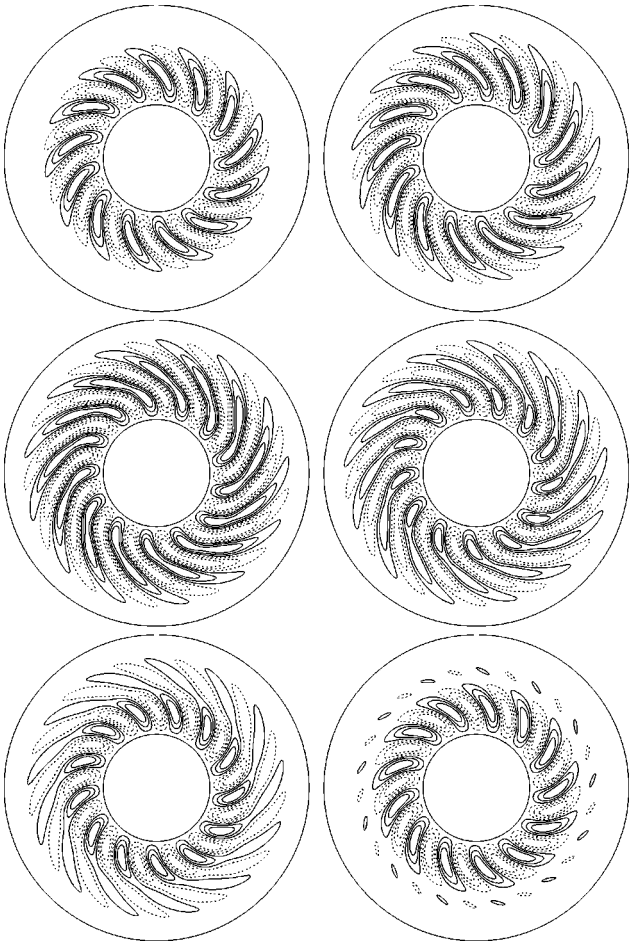

FIG. 6. Isovalues of ψ for vacillating oscillations for $E=10^{-5}$, $Ra=1.45\times Ra_c$, and $Pr=1$ (solid line for positive values of ψ, dashed for negative), with no-slip boundary conditions and explicit mode coupling. The graphs are equally spaced in time (from left to right and top to bottom). The time interval between consequetive graphs is 10^{-3} U.T. These six graphs cover a full period of the vacillation process.

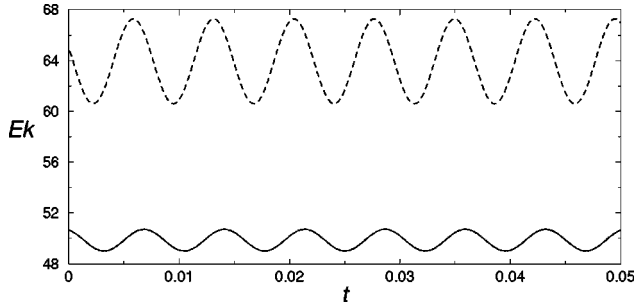

FIG. 5. Time oscillations of the kinetic energy for $E=10^{-5}$, $Ra=1.41\times Ra_c$, and $Pr=1$, with no-slip boundary conditions and explicit mode coupling. This parameter regime corresponds to vacillating oscillations. The energy of critical mode (Ek') is represented by a dashed line (it has been scaled by 0.4 for this graph), and the energy of mode $m=0$ (Ek_0) with solid line. The unit of time is the viscous time scale.

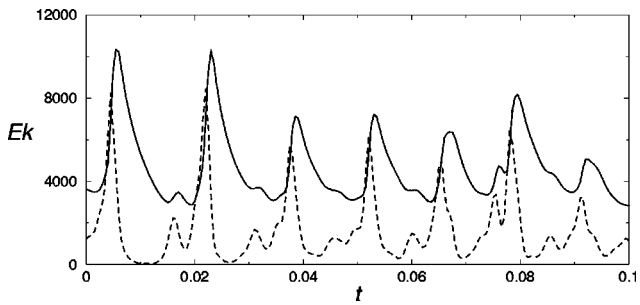

FIG. 7. Time oscillations of the kinetic energy for $E=10^{-5}$, $Ra=2.5\times Ra_c$, and $Pr=1$, with no-slip boundary conditions and explicit mode coupling. This parameter regime corresponds to relaxation oscillations. The energy of critical mode (Ek') is represented by a dashed line, and the energy of mode $m=0$ (Ek_0) by a solid line. The unit of time is the viscous time scale.

TABLE II. Critical parameters for the onset of vacillating flows (obtained with the explicit mode coupling method).

E	10^{-5}	10^{-6}	10^{-7}
	No-Slip		
$(Ra_{c_2}/Ra_c)-1$	0.41	0.25	0.01
	Stress-free		
$(Ra_{c_2}/Ra_c)-1$	0.44	0.29	0.01

The shearing action of the zonal flow is also well captured by this mode coupling approach (see, for example, Fig. 6) showing that all relevant physical ingredients remain present.

Chaotic oscillations and localized convection cannot, however, be reproduced with this approach since they require more complicated mode interactions. Relaxation oscillations are on the other hand obtained with this two-modes approach (e.g., Fig. 7 with no-slip boundary conditions). The threshold for this instability is, however, strongly affected by the severe truncation of such models. We will rely on this less demanding approach in the following sections.

3. Low Ekman number limit

The main advantage of the two-dimensional approach is that it enables us to investigate a wider range of parameters (the computing time is considerably reduced compared to three-dimensional simulations). We have investigated the onset of these solutions with time dependant behavior of the energy for decreasing Ekman numbers within the explicit mode coupling approach, with Prandtl number still set to the unity. Unexpectedly, this onset becomes closer to the onset of convection as the Ekman number is decreased. This applies to the entire sequence of bifurcations described previously. The onset for all of these time dependent instabilities converges towards the critical parameters for the onset of convection as the Ekman number decreases. Thus the range of Rayleigh number for which the convection is steady in amplitude vanishes for asymptotically small values of the Ekman number.

The values of the Rayleigh number for which the first solutions with time dependent energies are found are presented for both no-slip and stress-free boundary conditions in Table II. While the values reported in the table correspond to the first observation of a time dependent energy, for the lowest Ekman number, we directly obtained, for both sets of boundary conditions, the relaxation oscillations at a value of the Rayleigh number only 1% above critical.

Our results are expressed in terms of Ra/Ra_c, so that they are independent of the definition used for the Rayleigh number (even modified definitions such as RaE).

IV. DISCUSSION

In the graphs of Fig. 8, we show that for a given Ekman number the period of time oscillations of the kinetic energy decreases with increasing Rayleigh number. The growth rate increases as the Rayleigh number is pushed away from its critical value thus convection can recover before the zonal shear fully vanishes, resulting in a shortening of the relaxation oscillation period (see Fig. 8). As noted in Sec. III B 1, the zonal flow being much less constrained by stress-free boundary conditions, than no-slip boundary conditions, it decreases on a longer time scale, and the frequency of the relaxation oscillations at a given Rayleigh number is thus higher with the no-slip boundary conditions (see Fig. 8).

For all the investigated values of the Ekman number, we obtained only supercritical bifurcations for the onset of convection. Soward[2] demonstrated that for the original three-

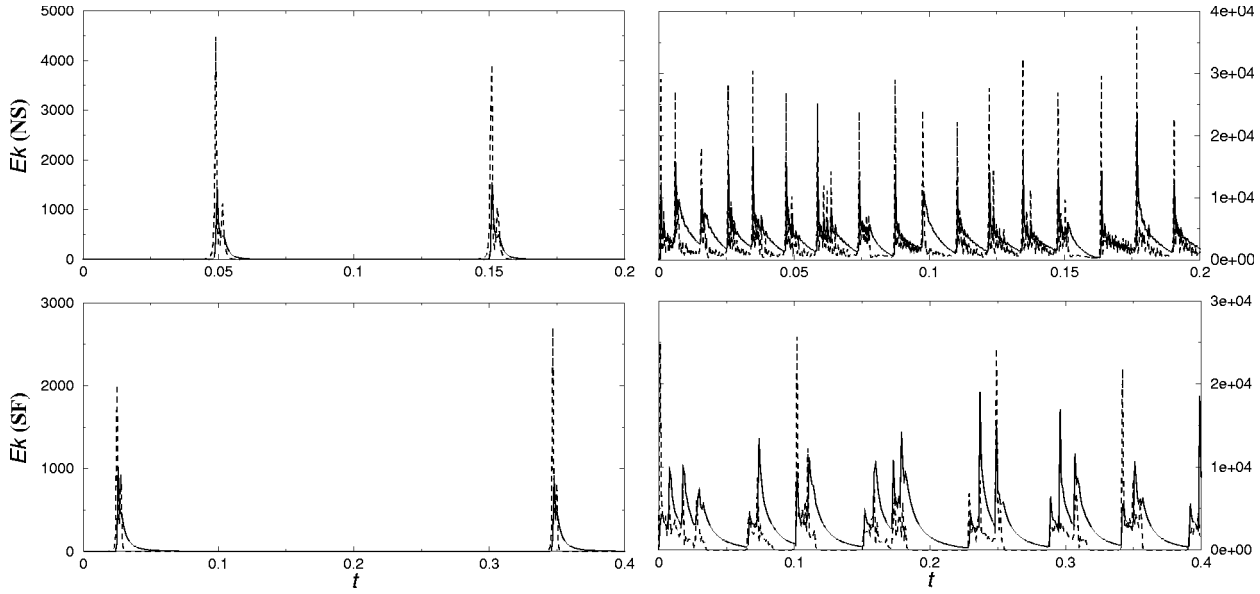

FIG. 8. Time oscillations of the kinetic energy for $E=10^{-7}$, $Pr=1$, on the left column $Ra=1.01\times Ra_c$, and on the right column $Ra=1.2\times Ra_c$. Results with no-slip boundary conditions are represented on the top graphs, and stress-free boundary conditions on the bottom graphs. This parameter regime yields relaxation oscillations. The energy of critical mode (Ek') is represented by a dashed line, and the energy of mode $m=0$ (Ek_0) by a solid line. The unit of time is the viscous time scale. Note that the range of time represented differs between both sets of boundary conditions.

dimensional (3D) problem, with rigid boundary conditions, the nonlinear effects would drive a zonal shear which could counter-act phase mixing and yield a subcritical bifurcation for the onset of convection. Like Chen *et al.*,[9] we have not observed any subcritical bifurcations despite the lower values of the Ekman number we have investigated. It is to be noted that the main nonlinearity invoked in Ref. 2 is the thermal wind, which is absent from our z-integrated simulations. The zonal flow in our simulations is driven by the Reynolds stress only. Furthermore the Ekman suction at the top and bottom of the columns was taken into account in Ref. 2, while neglected here. Despite the simplifications, the observation that the energy of convection can become time dependent extremely near the onset is an advance in our knowledge of the effects of the zonal flow of the asymptotic nature of the bifurcation associated with the onset of convection.

Relaxation oscillations in time evolve on typical time scales of fractions of the viscous diffusion time (decreasing fractions with increasing Rayleigh numbers). Similar relaxation oscillations but at much higher Rayleigh number and in a magnetohydrodynamic flow could suppress the convection in the Earth core (through the strong zonal shear) on a quasi-periodic basis. It is tempting to speculate, that relaxation oscillations modified by magnetic effects, could be related to the geomagnetic reversals occurring on Earth with a typical time scale of 100 kyr. This time scale, short compared to the viscous time scale, does not naturally appear from dimensional analysis. Relaxation oscillations are a good candidate to provide such time scales. A mechanism reducing the strength of convection would be compatible with the decrease in the geomagnetic field intensity observed between reversals.[22] Such relaxation oscillations in the magnetohydrodynamic regime, would clearly deserve further study.

ACKNOWLEDGMENTS

We thank Professor Andrew Soward, Professor Christopher Jones, and Steve Cole for helpful discussions in the course of this work. We are grateful to Dr. Julien Aubert for benchmarking our numerical code and to Christopher Finlay for many helpful corrections on an early version of this text. Numerical simulations were achieved on the IBM cluster at I.D.R.I.S., projects 30633, 40633.

[1] C. A. Jones, A. M. Soward, and A. I. Mussa, "The onset of thermal convection in a rapidly rotating sphere," J. Fluid Mech. **405**, 157 (2000).
[2] A. M. Soward, "On the finite amplitude thermal instability in a rapidly rotating fluid sphere," Geophys. Astrophys. Fluid Dyn. **9**, 19 (1977).
[3] F. H. Busse, "Thermal instabilities in rapidly rotating systems," J. Fluid Mech. **44**, 441 (1970).
[4] K. Zhang, "Spiralling columnar convection in rapidly rotating spherical fluid shells," J. Fluid Mech. **236**, 535 (1992).
[5] M. R. E. Proctor, "Convection and magnetoconvection in a rapidly rotating sphere," *Lectures on Solar and Planetary dynamo* (Cambridge University Press, Cambridge, 1994), p. 97.
[6] F. H. Busse and A. C. Or, "Convection in a rotating cylindrical annulus: Thermal Rossby waves," J. Fluid Mech. **166**, 173 (1986).
[7] A. C. Or and F. H. Busse, "Convection in a rotating cylindrical annulus. Part 2. Transition to asymmetric and vacillating flow," J. Fluid Mech. **174**, 313 (1987).
[8] E. Grote, F. H. Busse, and R. Simitev, "Buoyancy Driven Convection in Rotating Spherical Shells and Its Dynamo Action," *High Performance Computing in Science and Engineering*, edited by E. Krause and W. Jäger (Springer-Verlag, New York, 2001).
[9] C. X. Chen and K. Zhang, "Nonlinear convection in a rotating annulus with a finite gap," Geophys. Astrophys. Fluid Dyn. **96**, 499 (2002).
[10] J.-I. Yano, "Asymptotic theory of thermal convection in rapidly rotating systems," J. Fluid Mech. **243**, 103 (1992).
[11] J. Aubert, N. Gillet, and P. Cardin, "Quasigeostrophic models of convection in rotating spherical shells," Geochem. Geophys. Geosyst. **4**, 1052 (2003).
[12] E. Plaut and F. H. Busse, "Low-Prandtl-number convection in a rotating cylindrical annulus," J. Fluid Mech. **464**, 345 (2002).
[13] E. Dormy, A. M. Soward, C. A. Jones, D. Jault, and P. Cardin, "The onset of thermal convection in rotating spherical shells," J. Fluid Mech. **501**, 43 (2004).
[14] P. H. Roberts, "On the thermal instability of a rotating-fluid sphere containing heat sources," Philos. Trans. R. Soc. London, Ser. A **263**, 93 (1968).
[15] E. Grote and F. H. Busse, "Dynamics of convection and dynamos in rotating spherical fluid shells," Fluid Dyn. Res. **28**, 349 (2001).
[16] F. H. Busse, "Convective flows in rapidly rotating spheres and their dynamos action," Phys. Fluids **14**, 1301 (2002).
[17] K. Zhang, "Convection in a rapidly rotating spherical shell at infinite Prandtl number: Transition to vacillating flows," Phys. Earth Planet. Inter. **72**, 236 (1992).
[18] M. Schnaubelt and F. H. Busse, "Convection in a rotating cylindrical annulus. Part 3. Vacillating and spatially modulated flows," J. Fluid Mech. **245**, 155 (1992).
[19] A. Abdulrahman, C. A. Jones, M. R. E. Proctor, and K. Julien, "Large wavenumber convection in the rotating annulus," Geophys. Astrophys. Fluid Dyn. **93**, 227 (2000).
[20] K. Kumar, S. Fauve, and O. Thual, "Critical self-tuning: The example of zero Prandtl number convection," J. Phys. II **6**, 945 (1996).
[21] N. Brummell and J. Hart, "High Rayleigh number β-convection," Geophys. Astrophys. Fluid Dyn. **68**, 85 (1993).
[22] J.-P. Valet and L. Meynadier, "Geomagnetic field intensity and reversals during the last four million years," Nature (London) **366**, 234 (1993).